Physica Medica 42 (2017) 13–18

Contents lists available at ScienceDirect

Physica Medica

journal homepage: http://www.physicamedica.com

Technical note

Optimization of the exposure parameters in digital mammography using contrast-detail metrics

Leidy J. Rojas [a,b], Agnes M.F. Fausto [a,*], Anderson W. Mol [a], Fermin G. Velasco [a], P.O.S. Abreu [a], G. Henriques [a], T.A.C. Furquim [c]

[a] *Research Center in Radiation Sciences and Technologies, State University of Santa Cruz, Rodovia Jorge Amado km 16, Ilheus, Brazil*
[b] *Department of Basic Sciences, University Santo Tomas, Bucaramanga, Colombia*
[c] *Laboratory of Dosimetry, Institute of Physics, University of S. Paulo, S. Paulo, Brazil*

ARTICLE INFO

Article history:
Received 5 December 2016
Received in Revised form 18 June 2017
Accepted 1 August 2017

Keywords:
Digital mammography
Image quality
Contrast-detail analysis
Optimization

ABSTRACT

Purpose: Optimization studies in digital mammography aid to assure the image quality and radiological protection of the patient. The aim of this work is to test effectiveness and applicability of a method based on a Figure of Merit (FOM = $(IQF_{inv})^2$/AGD) to improve all the exposure parameters (Target/Filter combination, kVp and mAs) in order to improve the image acquisition technique that will provide the best compromise between image quality and the average glandular dose (AGD).

Methods: A contrast-detail analysis, employing the test object CDMAM, was carried out for the digital mammography unit manufactured by Lorad Hologic – model Selenia. We simulated two breast thicknesses using phantoms and a Figure of Merit as optimization tool, which includes an indicator of image quality, the IQF_{inv} and the average glandular dose. Images of the ACR and TORMAM phantoms were obtained with both, automatic and optimized exposure parameters. In order to compare the image quality, the SNR (Signal to Noise Ratio) was measured in each image.

Results: In the two phantoms, for both 4.5 and 7.5 cm thicknesses, the AGDs obtained with the optimized parameters show a reduction. In addition, the images obtained with the optimized exposure parameters, had the same or a better image quality when compared to the images obtained using the automatic mode.

Conclusions: The proposed optimization methodology proved to be an effective tool to improve the digital mammography unit, due to the use of objective metrics for evaluation and validation of the results.

1. Introduction

Breast cancer is the neoplasia that most affects women worldwide [1]. Early diagnosis is the most effective way to reduce mortality by this disease and increase patient survival [2]. The mammogram is the most used and recommended technique for this purpose [3]. An important issue in this topic relates to diagnostic image quality assessment. In a recent paper [4] authors report that mammography units that operate at an acceptable minimum for image quality, may have unacceptably low cancer detection rates. They conclude that the European image quality standards should be reviewed in order to raise the minimum level for image quality acceptance. Some authors [5,6] point out the potential of developed computational methods such as channelized Hoteling Observer and non-pre-whitening model observer with human visual system. With a structure detection performance close to the human observer, it is meant to assess clinical image quality.

To detect breast cancer early, mammographic images should exhibit a high contrast, which is not an easy task since the parts that compose the breast adipose and glandular tissue, have similar radiation attenuation coefficients. The diagnosis in mammography faces an additional challenge, that the breast tissues and pathological findings, have very close linear attenuation coefficients within the energy range used in mammography [7]. The Target/Filter combination and the energy chosen in the image acquisition technique affect the contrast between tissues types. In the radiological image, the difference between the linear attenuation coefficients of radiation in each tissue tends to increase with decreasing energy, usually for energies lower than 30 keV [8]. The presence of microcalcification is an indication of the possible development of breast cancer [9–11]. Although these structures have higher contrast than the masses, microcalcification can occur in a very small size and the noise affects their visualization. Increasing the current-time

* Corresponding author.
E-mail address: amffausto@uesc.br (A.M.F. Fausto).

http://dx.doi.org/10.1016/j.ejmp.2017.08.001
1120-1797/

product (mAs) in the mammographic unit reduces the noise in the image, but this simultaneously increases the radiation dose in the patient. Therefore, the determination of the optimum X-ray spectrum for mammography involves a careful compromise between image contrast, radiation dose, and image statistical noise [12]. The aim of the optimization of radiodiagnosis techniques is to provide the best compromise between image quality and radiation dose, related to the principles of radiation protection [13]. In order to perform the mammographic examination, it is necessary and challenging to develop techniques, which are capable to differentiate healthy tissue from the radiological signs of breast cancer, in order to optimize the relationship between image quality and radiation dose to the patient.

The Figure of Merit (FOM) is a tool used in optimization studies in radiology, and it is defined using metrics of image quality and radiation dose. Several FOM definitions have been applied in order to optimize mammography systems [14–18]. The results of these studies indicate that the parameters selected by the AEC mode, Target/Filter combination, kVp and mAs do not necessarily are the most suitable for the achievement of mammograms of different breast thicknesses and compositions [19].

In light of the above, it is important to perform specialized studies of optimization techniques for digital mammography and individualized studies for each type of mammography system [20]. The aim of this work is to test effectiveness and applicability of a recently proposed method [21], based on a Figure of Merit ($FOM = (IQF_{inv})^2/AGD$) to optimize all the exposure parameters (Target/Filter combination, kVp and mAs) in a different digital mammography equipment, and for distinct breast thicknesses.

2. Materials and methods

The optimization methodology was implemented in three stages, shown in Fig. 1. The first stage was conducted in three parts. In part one a characterization performance of the mammography unit in question was carried out. This included the acceptance tests at the time of installation as well as periodic quality control tests in accordance with Brazilian regulatory guidelines [22].

The present work was carried out using the digital mammography Hologic Selenia model, installed at the Research Center in Radiation Sciences and Technologies (CPqCTR) of the State University of Santa Cruz (UESC), Bahia, Brazil.

Thereafter, during the second part, the FOM proposed by Fausto [21] (Eq. (1)) was used for the optimization of the exposure parameters: target/filter combination (T/F), kilovoltage peak (kVp) and the current-time product (mAs). The FOM is calculated by relating two parameters involved in the image acquisition process: image quality in terms of inverted image quality factor (IQF_{inv}) and the average glandular dose (AGD).

$$FOM = (IQF_{inv})^2/AGD \tag{1}$$

We used the Contrast-Detail Mammography Phantom (CDMAM, type 3.4) [23] to obtain the required images in order to calculate the IQF_{inv}. The CDMAM-phantom consists of an aluminum base with golden disks, which is attached to a Plexiglas cover. It has a matrix of square cells, 16 columns and 16 rows, with disks of variable diameter (from 0.06 to 2.00 mm) and thickness (from 0.03 to 2.00 μm). Each square contains two identical disks, one in the center and one in a randomly chosen corner. The detection of disks by the observer is evaluated as percentages of correct detections per image.

The CDMAM enabled us to obtain the system's contrast-detail curve, in order to determine the visibility threshold. This curve is related to the detection capability of the smallest structures depending on the exposure parameters. The IQF_{inv} was obtained using the test object CDMAM (Contrast-Detail Mammography), which determines the contrast (thickness in μm) of the visibility threshold C_i^{th} in the image of the object as a function of the detail (diameter in mm) D_i. The IQF_{inv} is calculated according to Eq. (2).

$$IQF_{inv} = \frac{100}{\sum_{i=1}^{16} C_i^{th} \cdot D_i} \tag{2}$$

A quantitative and objective evaluation of the images obtained using the CDMAM 3.4 was performed using the software CDMAM analyzer V1.2 of Artinis [23].

The use of IQF_{inv} is appropriate due the importance of detection of low contrast structures (masses) and details of few diameters (microcalcifications) in the mammography examination.

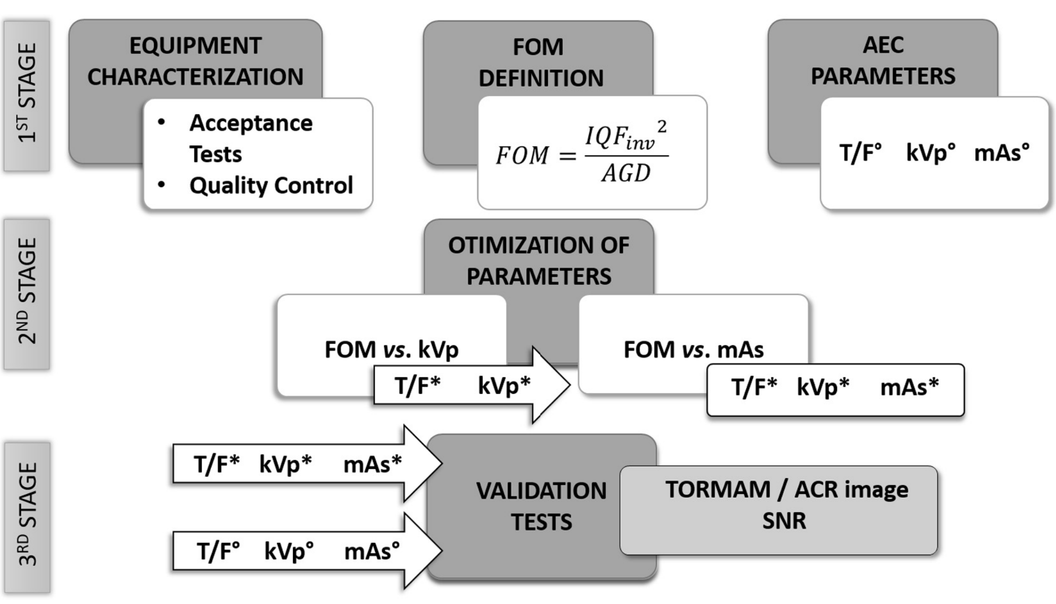

Fig. 1. Methodological framework.

In the optimization process, we must take the radiation risk into account, which is associated to the AGD because the glandular tissue is the most radiosensitive breast tissue. The AGD was calculated using Eq. (3), according to the methodology proposed by the International Atomic Energy Agency (IAEA) [24].

$$AGD = g_t c_t s K_{i,t} [\mathrm{Gy}] \quad (3)$$

In which:

$K_{i,t}$ is the entrance air kerma at the surface measured without backscatter;
s is the correction factor that depends on the target-filter combination;
c_t is the conversion factor which allows for the glandularity of a standard breast of thickness t;
g_t is the factor that converts the $K_{i,t}$ in AGD for a breast with 50% of glandular tissue.

The measure of $K_{i,t}$ was performed according to the methodology proposed in the European Protocol on Dosimetry in Mammography [25], using the dosimetry set composed by the 9095 model Radcal electrometer coupled to the ionization chamber (IC) dedicated to mammography 10x9-6M model. Calculation of the AGD was carried out using the formula proposed in the European Protocol [26] and by the International Atomic Energy Agency [24]. The values used for: s, c_t and g_t are taken from Dance et al. [27] in accordance with the corresponding T/F set used and the standard 50% glandularity breast.

In the third part of stage one, we used the phantom from the American College of Radiology (ACR), which is actually a standard for image quality evaluations, with a thickness of 4.5 cm and 50/50 composition (glandular/fatty tissue), and also an anthropomorphic phantom (TORMAM). The exposure parameters (T/F°, kVp° and mAs°) were obtained using the automatic exposure control (AEC) mode with both phantoms using two different breast thicknesses: 4.5 cm and 7.5 cm (adding PMMA plates).

The second stage was performed in two parts as shown in Fig. 1. In the first part, the objective was to find the optimal kVp and T/F combination. For this purpose the FOM was calculated for each kVp value in the range of 25–35 kVp that was available in the mammography unit.

The value of IQF_{inv} increases with the mAs when the other parameters are maintained fixed. Thus, it was necessary to define a criterion for determining mAs in order to obtain images in which the IQF_{inv} values could be compared. The criterion suggested by Ranger et al. [28] was applied to use the current-time products, so that the image's mean pixel values (MPV), is kept close to the value recommended by the manufacturer. In the case of the Selenia mammography unit, MPV is around 350 ± 5% [29]. The FOM *vs.* kVp curves were plotted for the two T/F combinations of the equipment: Mo/Mo and Mo/Rh.

For each filter the best fit curve was found, and then selected the one that showed higher FOM value as the optimal filter. The optimum kVp was selected from the peak of the curve FOM *vs.* kVp using the chosen filter. The FOM value was calculated for different mAs but maintaining a constant signal level (MPV) in the images.

The mAs optimization was based on the results of the optimal kVp* and T/F* combination. The FOM *vs.* mAs curve was then plotted and the mAs with the maximum value of FOM in the fitted curve, was selected as the optimal mAs*. We have obtained the optimized exposure parameters at the end of this stage.

The aim of the third stage of the methodology is to evaluate the results of the optimization, using the TORMAM anthropomorphic phantom. The TORMAM images obtained with optimized exposure parameters (T/F*, kVp*, mAs*) were compared with the corresponding images for the AEC parameters. The SNR (Signal to Noise Ratio) were calculated from the phantom images in order to validate the optimization results. In addition, the same tests were performed with the standard ACR phantom.

3. Results and discussion

3.1. Quality assurance of the mammography unit

The acceptance tests and the periodic quality control tests were carried out. In that way, the constancy of the equipment performance throughout the period of this study was ensured. In all the tests, the equipment presented performance characteristics in accordance with regulatory standards.

3.2. Automatic image exposure parameters

Table 1 shows the values of the automatic image exposure parameters selected by the AEC system for two breast thicknesses from the ACR and TORMAM phantoms.

3.3. Optimization of the exposure parameters

3.3.1. Optimization of kVp

The kVp optimization was performed using the FOM defined in Eq. (1). The IQF_{inv} *vs.* kVp (Fig. 2) and FOM *vs.* kVp (Fig. 3) curves were plotted for a thickness of 4.5 cm and 7.5 cm of compressed breast. Comparison and analysis are also indicated for the points corresponding to the IQF_{inv} using the parameters obtained in the AEC mode for the ACR phantom.

In the Fig. 2, a decrease of IQF_{inv} is observed with the increase of kVp. This is related with the fact that in order to guarantee the same level of exposure (MPV) in the detector, it is necessary to select successively smaller values of mAs with the growth of kVp. Lower values of mAs decrease both the dose and IQF_{inv}. We observed from the Table 3, that the value of the IQF_{inv} in the AEC mode for de ACR phantom is slightly higher than the optimized for both breast thicknesses. However, considering the uncertainties, these values are almost the same. On the other hand, with the optimization, the doses were reduced considerably compared to the AEC mode. For the 4.5 cm and 7.5 cm breast thickness the doses with the optimized parameters show a reduction of 26% and 16%, respectively.

Fig. 3 shows the FOM *vs.* kVp curves obtained for each assessed breast thickness. In general, the functions of Gaussian type show the best fitted curves for each T/F combination, through which the kVp with the maximum FOM value was determined. Fig. 3(a) shows the optimization curves for 4.5 cm breast thickness and the result of the FOM for the parameters selected by the AEC for the ACR phantom. It is observed that the Mo/Rh curve is the one with the highest FOM value in the entire voltage range, while the choice of the AEC mode for this particular breast thickness was the Mo/Mo combination. The T/F combination selected by the mammography unit for compressed breast thicknesses below 6.5 cm is usually Mo/Mo. The Mo/Rh combination is not commonly used because the Rh filter allows a greater fraction of photons with higher energies compared with the spectrum resulting from the Mo/Mo combination. The most energetic photons tend to reduce the contrast, because for high-energy photons, the linear attenuation coefficients of the different breast tissues are closer. The kiloVolt-peak of 30.8 kVp is the center value of the Mo/Rh curve and corresponds to the highest FOM value.

Fig. 3(b) shows the curve optimization for breast thickness of 7.5 cm and the result of the FOM in the AEC parameters for de ACR phantom. The kVp value, which reaches the highest FOM for

Table 1
Parameters selected by the AEC for the ACR and TORMAM phantoms.

Exposure parameters[1]	ACR		TORMAM	
	Thickness		Thickness	
	4.5 cm	7.5 cm	4.5 cm	7.5 cm
T/F	Mo/Mo	Mo/Rh	Mo/Mo	Mo/Rh
kVp	28	32	30	34
mAs	75	160	62	145

[1] Parameters selected with Auto-Filter exposure mode.

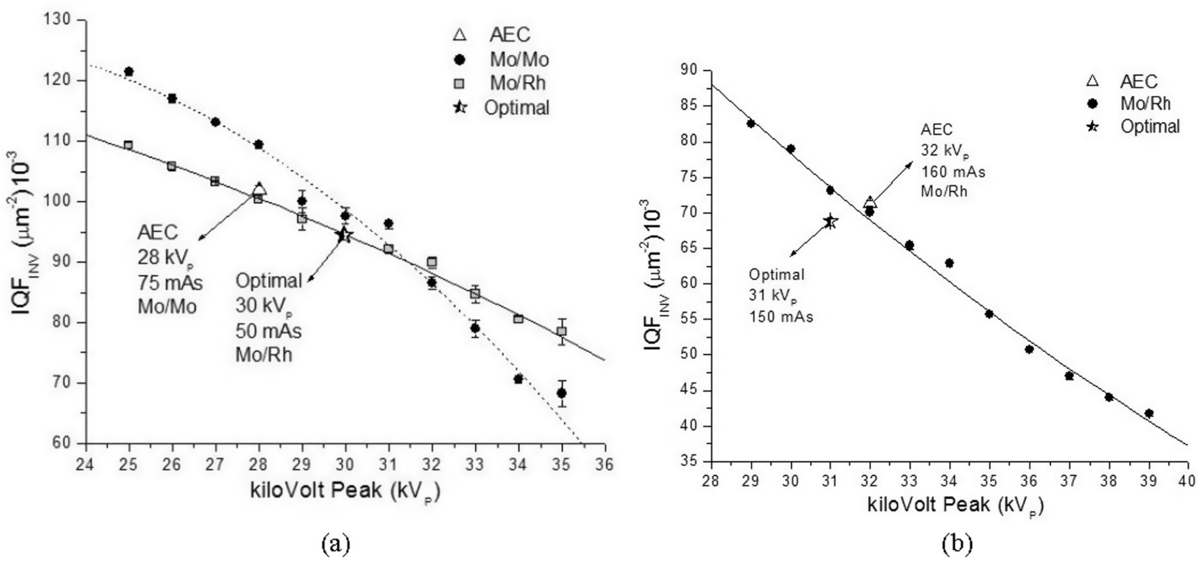

Fig. 2. IQF$_{inv}$ *vs.* kVp curves (a) For 4.5 cm of breast thickness (b) For 7.5 cm of breast thickness.

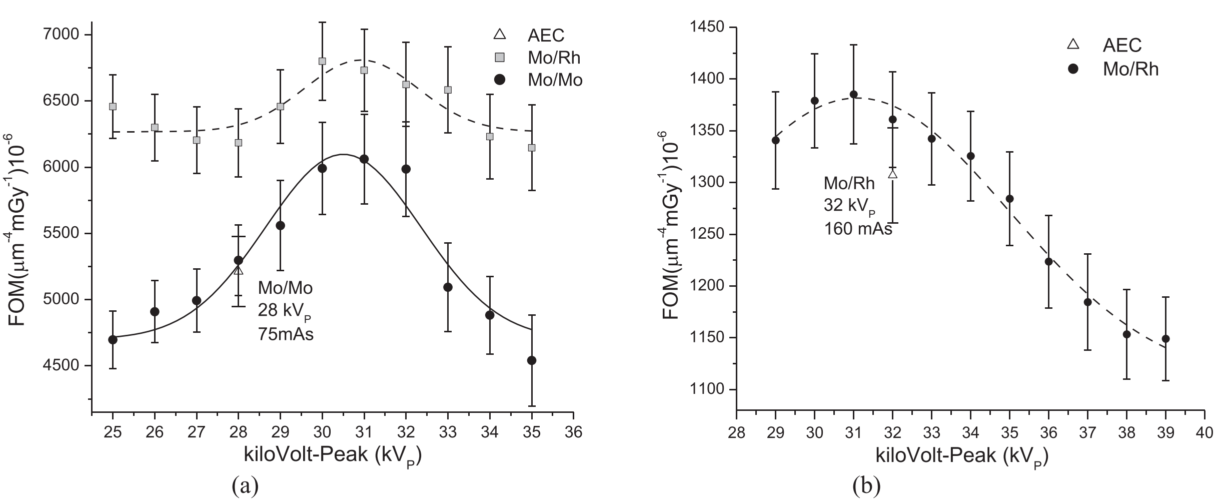

Fig. 3. FOM *vs.* kVp curves (a) For 4.5 cm of thickness (b) For 7.5 cm of thickness.

this thickness is 31.1 kVp, which differs from the value selected by the AEC (32 kVp).

3.3.2. Optimization of mAs

The mAs optimization was performed seeking the maximum of the FOM *vs.* mAs curve, using the optimal kVp and T/F combination. The optimal kVp found for the two breast thicknesses were non-integer values of voltage, namely 30.8 kVp for 4.5 cm thickness and 31.1 kVp for 7.5 cm of thickness. In the mammography unit, it is only possible to select full voltage values. Hence, the FOM *vs.* mAs curve was plotted in each case for the two voltages closest to the optimal kVp values, i.e. 30 and 31 kVp for the thickness of 4.5 cm and 31 and 32 kVp for the thickness of 7.5 cm as shown in Fig. 2. For each kVp value, the corresponding FOM *vs.* mAs curve was plotted, as shown in Fig. 4. For the thickness of 4.5 cm, the 30 kVp curve showed the maximum value of FOM at 50 mAs (Fig. 4(a)). For the thickness of 7.5 cm, the curve with 31 kVp showed the maximum value of FOM with 150 mAs (Fig. 4(b)).

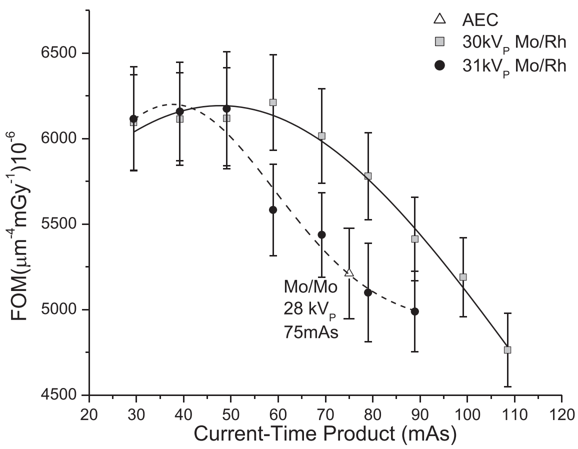

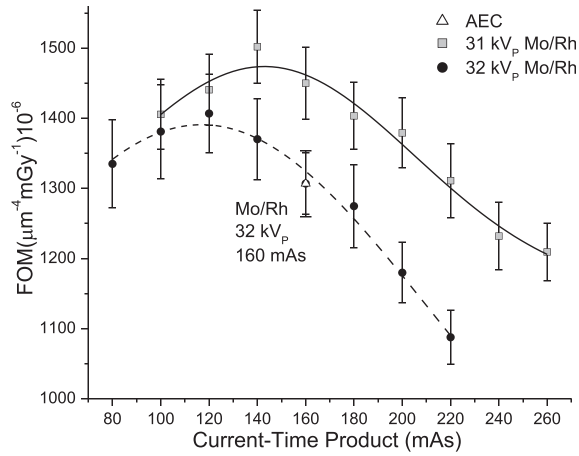

Fig. 4. FOM *vs.* mAs curves (a) For 4.5 cm of thickness (b) For 7.5 cm of thickness.

Table 2
The exposure parameters, ⟨SNR⟩ and AGD for the two assessed thicknesses, comparing results for the optimized and AEC configurations for TORMAM phantom.

Physical exposure parameters	4.5 cm of Thickness		7.5 cm of Thickness	
	AEC	Optimized	AEC	Optimized
T/F	Mo/Mo	Mo/Rh	Mo/Rh	Mo/Rh
kVp	30	30	34	31
mAs	62	50	145	150
AGD (mGy)	1.94 ± 0.10	1.47 ± 0.07	3.81 ± 0.13	3.26 ± 0.13
⟨SNR⟩	27.6 ± 1.5	44.9 ± 0.4	39.9 ± 0.8	38.6 ± 0.5

Table 3
The exposure parameters, ⟨SNR⟩ and AGD for the two assessed thicknesses, comparing results for the optimized and AEC configurations for ACR phantom.

Physical exposure parameters	4.5 cm of Thickness		7.5 cm of Thickness	
	AEC	Optimized	AEC	Optimized
T/F	Mo/Mo	Mo/Rh	Mo/Rh	Mo/Rh
kVp	28	30	32	31
mAs	75	50	160	150
AGD (mGy)	1.99 ± 0.09	1.47 ± 0.07	3.90 ± 0.13	3.26 ± 0.13
⟨SNR⟩	52.4 ± 1.2	52.0 ± 0.6	45.6 ± 0.6	43.8 ± 0.4

Finally, the physical exposure parameters optimized for 4.5 cm breast thickness are the Mo/Rh combination with 30 kVp and 50 mAs. The Mo/Rh combination with 31 kVp and 150 mAs are the optimized parameters for 7.5 cm of breast thickness.

4. Validation tests

For the validation tests, a set of TORMAM phantom images using the combinations of the optimized parameters was used. Then, we compared the optimized TORMAM images with the TORMAM images obtained in the AEC mode. JiveX [dv] Viewer Personal Edition software was used to obtain the SNR values. It was selected a ROI in three separated regions of the image, positioned over the locations with PMMA and without structures. An average ⟨SNR⟩ value was obtained for each image. The SNR metric was then used so to compare image quality.

Tables 2 and 3 show the results for the assessed metric to the AEC mode and the optimized parameters, for TORMAM and ACR phantoms respectively. The TORMAM images obtained with the optimized parameters for 4.5 cm of thickness have a higher ⟨SNR⟩ value compared to the AEC images within the range of uncertainty involved. Also, the AGD calculated with the optimized parameters is 24% below the AGD calculated for the AEC parameters. Thus, mammograms performed in breast with 4.5 cm thickness, using the optimized parameters can provide results with better image quality, than those obtained with the AEC parameters, with a significant dose reduction.

For the compressed breast thickness of 7.5 cm, the value of the SNR for the optimized image had the same value compared with the AEC image, within the range of uncertainties involved. Furthermore, the AGD calculated with the optimized parameters is about 14% below the one calculated for the AEC parameters. This fact suggests that the parameters obtained within the optimization methodology, as proposed in this work, also outperforms the AEC parameters for this breast thickness.

The results obtained with the ACR phantom are consistent with those obtained with the TORMAM anthropomorphic phantom. Indeed, in both tests, it was found that the optimization of the exposure parameters allowed for a significant reduction of the dose, maintaining almost the same value of the image quality index for the large breast thickness. Notwithstanding, for the

4.5 cm thickness breast, the TORMAM and ACR tests showed distinct results for the image quality index. That is, the SNR metric result of TORMAM image was able to show more clearly that the proposed optimization achieved a significant improvement in the image quality, compared to the image obtained in the AEC mode.

According to Mackenzie et al. [4], the clinical effectiveness of the task of detecting clusters of calcifications in mammography is linked to the evaluation of image quality using the CDMAM phantom. This conclusion also coincides with our previous results reported in Fausto et al. [21], based on this FOM that also uses CDMAM. Where the optimization of the exposure parameters for the 4.5 cm breast, presented better results for the detection of microcalcifications in analyses performed by the radiologists using TORMAM phantom images.

According to Borg et al. [14], the FOM defined as the ratio of the CNR^2 to the AGD seems to be the most appropriate and suitable for intra-system comparison. However, this authors point out that CNR, that use raw images, may also be an unreliable metric, because of image post processing or corrective algorithms. They defended the opinion that the mammography inter-system comparison could be made possible by replacing the CNR in the FOM definition by a different image quality indicator, depending less on manufacturer but rather gauging image quality holistically.

In the present research we applied a FOM, previously reported by us, that can use both: processed and raw image with equivalent results. The application of the proposed methodology and its independence of image processing suggest its potential applicability in inter-system comparisons. However, a more extensive research should be done to study this possibility.

5. Conclusions

- Based on the results of the optimization, it is possible to conclude that in the assessed digital mammography unit it is possible to obtain images with improved quality and lower radiation dose.
- The proposed optimization methodology showed to be an effective tool to optimize the digital mammography unit due to the use of objective metrics for evaluation and validation of results.

Acknowledgments

This work was supported by the cooperation program of the Organization of American States (OAS) with the Grupo Coimbra de Universidades Brasileiras (GCUB), the Coordination of Improvement of Higher Level Personnel (CAPES), Funding of Studies and Projects (FINEP), Foundation for Research Support of the State of Bahia (FAPESB), and the State University of Santa Cruz (UESC).

References

[1] World Health Organization. Breast cancer: estimated incidence, mortality and prevalence worldwide in 2012. GLOBOCAN 2012. http://globocan.iarc.fr/Pages/fact_sheets_cancer.aspx (accessed December 12, 2015).
[2] Michaelson J, Satija S, Moore R, Weber G, Halpern E, Garland A, et al. The pattern of breast cancer screening utilization and its consequences. Cancer 2002;94:37–43. http://dx.doi.org/10.1002/cncr.10154.
[3] Yaffe MJ, Mainprize JG, Jong RA. Technical developments in mammography. Health Phys 2008;95:599–611. http://dx.doi.org/10.1097/01.HP.0000327648.42431.75.
[4] Mackenzie A, Warren LM, Wallis MG, Given-Wilson RM, Cooke J, Dance DR, et al. The relationship between cancer detection in mammography and image quality measurements. Phys Med 2016;32:568–74. http://dx.doi.org/10.1016/j.ejmp.2016.03.004.
[5] Bouwman RW, van Engen RE, Broeders MJM, den Heeten GJ, Dance DR, Young KC, et al. Can the non-pre-whitening model observer, including aspects of the human visual system, predict human observer performance in mammography? Phys Med 2016;32:1559–69. http://dx.doi.org/10.1016/j.ejmp.2016.11.109.
[6] Bouwman RW, Goffi M, van Engen RE, Broeders MJM, Dance DR, Young KC, et al. Can the channelized Hotelling observer including aspects of the human visual system predict human observer performance in mammography? Phys Med 2017;33:95–105. http://dx.doi.org/10.1016/j.ejmp.2016.12.015.
[7] Chen RC, Longo R, Rigon L, Zanconati F, De Pellegrin A, Arfelli F, et al. Measurement of the linear attenuation coefficients of breast tissues by synchrotron radiation computed tomography. Phys Med Biol 2010;55:4993–5005. http://dx.doi.org/10.1088/0031-9155/55/17/008.
[8] Johns Paul C, Yaffe Martin J. X-ray characterisation of normal and neoplastic breast tissues. Phys Med Biol 1987;41:315.
[9] Morgan MP, Cooke MM, McCarthy GM. Microcalcifications associated with breast cancer: an epiphenomenon or biologically significant feature of selected tumors? J Mammary Gland Biol Neoplasia 2005;10:181–7. http://dx.doi.org/10.1007/s10911-005-5400-6.
[10] Cox RF, Hernandez-Santana A, Ramdass S, McMahon G, Harmey JH, Morgan MP. Microcalcifications in breast cancer: novel insights into the molecular mechanism and functional consequence of mammary mineralisation. Br J Cancer 2012;106:525–37. http://dx.doi.org/10.1038/bjc.2011.583.
[11] Baker R, Rogers KD, Shepherd N, Stone N. New relationships between breast microcalcifications and cancer. Br J Cancer 2010;103:1034–9. http://dx.doi.org/10.1038/sj.bjc.6605873.
[12] Qian X. Fundamentals of digital mammography. In: Markey MK, editor. Phys. mammographic imaging. Boca Raton: Taylor & Francis Group; 2013. p. 3–10.
[13] European Commission. Council Directive 97/43/Euratom of 30 June 1997 on health protection on individuals against the dangers of ionizing radiation in relation to medical exposure, and repealing Directi ve 84/466/Euratom; 1997:22.
[14] Borg M, Badr I, Royle G. The use of a figure-of-merit (FOM) in digital mammography. Radiat Prot Dosimetry 2012;151:81–8.
[15] Baldelli P, Phelan N, Egan G. Investigation of the effect of anode/filter materials on the dose and image quality of a digital mammography system based on an amorphous selenium flat panel detector. Br J Radiol 2010;83:290–5. http://dx.doi.org/10.1259/bjr/60404532.
[16] Kanaga KC, Yap HH, Laila SE, Sulaiman T, Zaharah MSA. A critical comparison of three full field digital mammography systems using figure of merit. Med J Malaysia 2010;65:119–22.
[17] Samei E, Dobbins JT, Lo JY, Tornai MP. A framework for optimising the radiographic technique in digital X-ray imaging. Radiat Prot Dosimetry 2005;114:220–9. http://dx.doi.org/10.1093/rpd/nch562.
[18] Williams MB, Raghunathan P, More MJ, Seibert JA, Kwan A, Lo JY, et al. Optimization of exposure parameters in full field digital mammography. Med Phys 2008;35:2414–23. http://dx.doi.org/10.1118/1.2912177.
[19] Tomal A, Perez AMMM, Silva MC, Poletti ME. Experimental evaluation of the image quality and dose in digital mammography: influence of X-ray spectrum. Radiat Phys Chem 2015;116:282–6. http://dx.doi.org/10.1016/j.radphyschem.2015.04.019.
[20] Furquim TC, Nersissian DY. Estudos de otimização de dose e qualidade de imagem em processos de transição tecnológica em mamografia Studies of dose optimization and image quality in technological transition in mammography. Rev Bras Fis Médica 2011;4:11–4.
[21] Fausto AMF, Lopes MC, de Sousa MC, Furquim TAC, Mol AW, Velasco FG. Optimization of image quality and dose in digital mammography. J Digit Imaging 2017;30:185–96. http://dx.doi.org/10.1007/s10278-016-9928-3.
[22] ANVISA. Aprova o regulamento técnico que estabelece as diretrizes básicas de proteção radiológica em radiodiagnóstico médico e odontológico, dispõe sobre o uso de raios-X diagnóstico em todo território nacional e dá outras providências; 1998:1998.
[23] Thijssen M. et al. Manual contrast-detail phantom CDMAM 3.4 & CDMAM Analyser software V1.2; 2010.
[24] IAEA. Quality assurance programme for digital mammography. Vienna; 2011.
[25] European Commission. European protocol on dosimetry in mammography. EUR 1623 EN; 1996.
[26] European Commision. European guidelines for quality assurance in breast cancer screening and diagnosis; 2006:4th ed.
[27] Dance DR, Young KC, Van Engen RE. Further factors for the estimation of mean glandular dose using the United Kingdom, European and IAEA breast dosimetry protocols. Phys Med Biol 2009;54:4361–72. http://dx.doi.org/10.1088/0031-9155/54/14/002.
[28] Ranger NT, Lo JY, Samei E. A technique optimization protocol and the potential for dose reduction in digital mammography. Med Phys 2010;37:962–9. http://dx.doi.org/10.1118/1.3276732.
[29] Oduko J, Young K. NHSBSP Equipment Report 0901. Review of measurements on full field digital mammography systems. London; 2009.